Received: 29 August 2021 | Revised: 19 January 2022 | Accepted: 14 February 2022

IET Circuits, Devices & Systems

DOI: 10.1049/cds2.12113

The Institution of Engineering and Technology WILEY

ORIGINAL RESEARCH

Frequency generator demonstration using half mode Substrate Integrated Waveguide (SIW) structures for chipless Radio Frequency Identification (RFID) reader

Vijay Sharma[1] | **Mohammad Hashmi**[1,2]

[1]Electronics and Communication Engineering Department, IIIT-Delhi, New Delhi, India

[2]School of Engineering and Digital Sciences, Nazarbayev University, Nur-Sultan, Kazakhstan

Correspondence

Vijay Sharma, Electronics and Communication Engineering Department, IIIT-Delhi, New Delhi, 110020, India.
Email: vijays@iiitd.ac.in

Funding information

Nazarbayev University Collaborative Research Program (CRP), Grant/Award Number: 021220CRP0222; Nazarbayev University Faculty-Development Competitive Research Grants Program (FDCRGP), Grant/Award Number: 110119FD4515

Abstract

A frequency generator based on the forward coupler principle is proposed. The proposed design, intended for high-frequency applications, uses Half-Mode Substrate Integrated Waveguide structure to realise the forward coupler. It thus achieves compactness, requiring approximately half the area compared to Substrate Integrated Waveguide structures, and supports non Transverse Electromagnetic (TEM) functionality. The non-TEM environment provides the flexibility to use the frequency generator for chipless Radio Frequency Identification readers in the sub-GHz band and mm-wave range. Full-wave simulations and the subsequent measurements on a prototype developed on Rogers 3006 substrate performed for the forward coupler resonators and frequency generator validate the proposed design concept.

KEYWORDS

radiofrequency identification, radiofrequency oscillators

1 | INTRODUCTION

The chipless Radio Frequency Identification (RFID) tag is the subcategory of passive RFID [1, 2]. In the chipless system, the RFID reader reads the backscattered response of the chipless tags for encoding purposes. It detects the frequency spectrum of the received signal and extracts the tag signature. The detection range and backscattered signal strength are crucial factors in defining the chipless RFID system's suitability in any application [3]. The backscattered response of chipless RFID is lower, as it is highly affected by distance and noise, and hence the chipless RFID system is mainly suitable for short-range communication applications. Furthermore, the RFID reader holds a crucial role in the overall cost and performance of the chipless RFID systems considering that the chipless RFID tags can be printed on the low-cost substrate and paper [4].

Recent works in this domain have been primarily in the Ultra-Wideband regime and focussed on the cost reduction of the tag [5–7]. The size of the chipless tags can be further reduced by choosing a higher operating frequency and mm wave of the RFID systems. However, they come at the increased cost of the reader's frequency generating unit [8]. Furthermore, frequency-dependent transmission faces higher losses and dispersion at a higher frequency according to Kramers-Kronig relations [9]. Another critical factor in the frequency generating units of RFID readers is the phase noise at high frequencies [10, 11]. There have been a renewed interest in Substrate Integrated Waveguide (SIW) structures as they have the potential to address the concerns associated with high-frequency devices [12, 13]. The SIW is a transition between the microstrip line and Dielectric Filled Waveguide (DFW). The DFW is converted to SIW with the help of vias in the sidewalls of the waveguide, as presented in Figure 1. One of the key features of the SIW structures is the high-quality factor [14], which enables low phase noise [15], high power capability, and low insertion loss [16]. Its compatibility with standard fabrication processes makes a promising waveguide solution for a large number of microwave applications. Substrate Integrated Waveguide circuits allow planner and non-

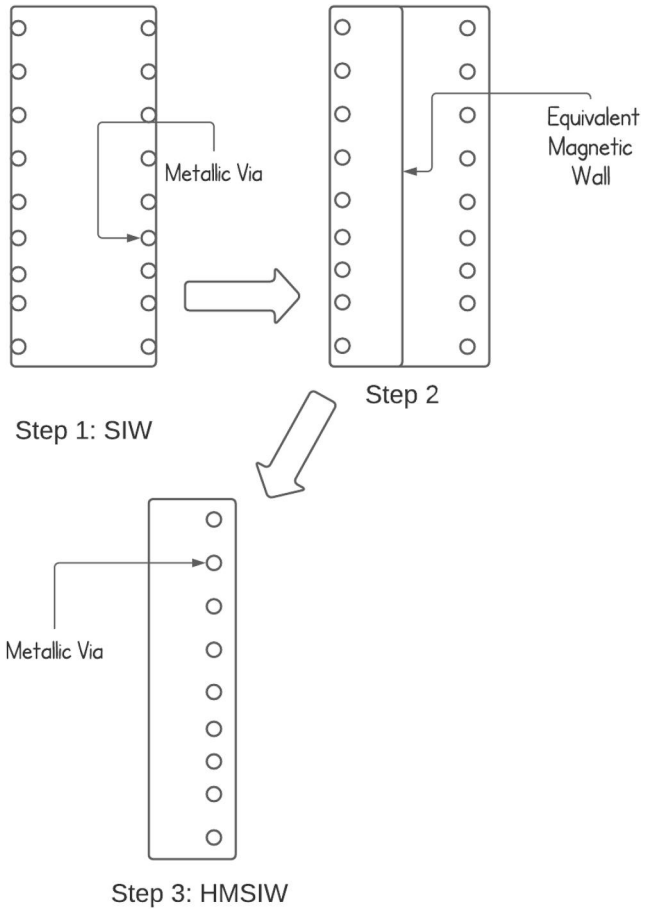

FIGURE 1 Transition of Substrate Integrated Waveguide (SIW) structure into Half-Mode SIW (HMSIW) structure

planner structures within the same substrate [17, 18] and lead to the design of low-cost millimetre-wave transceivers.

A number of reports on frequency generators or oscillators based on SIW structures with fixed oscillation frequencies exist in literature [19–21]. However, these oscillators often suffer from large size and design complexity and cannot be tuned continuously. However, these issues can be overcome by Transverse Electromagnetic (TEM) C-section structures [22]. But C-section structures are difficult to realise at higher frequencies due to large coupling while achieving more substantial dispersion. Similarly, the SIW structure augmented with an external amplifier enables the design of a low-cost microwave oscillator [21]. However, the presence of an external amplifier makes the size of this oscillator large.

The size of the SIW structure is a significant concern, and the size can be reduced using Folded Substrate Integrated Waveguide (FSIW) [23]. However, it employs a multilayer structure which increases the costs and the fabrication complexity. A Half-Mode Substrate Integrated Waveguide (HMSIW) is an excellent alternative to SIW and FSIW, which reduces the width of the SIW by 50%, keeping all the advantages of the full mode SIW structure [24], as shown in Figure 1. High frequency and mm wave RFID reader opens a new path for chipless RFID to reduce the size further.

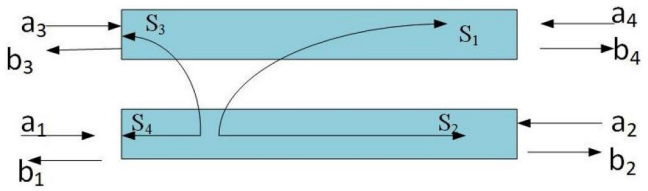

FIGURE 2 Signal flow graph of a four-port coupler

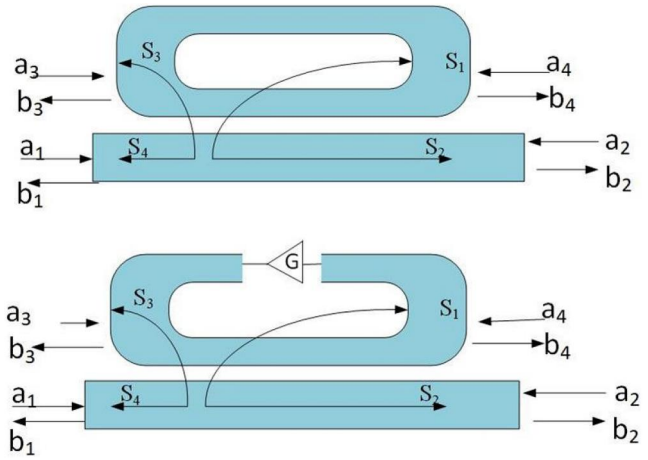

FIGURE 3 Flow graph of two-port forward coupler passive ring (up). Passive ring with a gain element inside the ring (below)

Therefore, this paper proposes a novel HMSIW frequency generator for high-frequency chipless RFID readers using the forward coupler concept. Half-Mode Substrate Integrated Waveguide is capable of propagating guided waves in only half-width of standard SIW and requires slightly more than half of the width of SIW to operate with the same cutoff frequency [24]. The waveguide structure helps to operate the system at higher frequencies without losses. The frequency generator using the HMSIW structure has been prototyped on the Rogers 3006 substrate, and the measurements and simulation results show excellent transmission and oscillation results under various conditions.

The paper explains the mathematical model and design of the HMSIW structures for the forward coupler in Section 2. Section 3 discuss the measurements and characterisation of the HMSIW forward coupler resonator, and Section 4 presents the oscillation analysis of the frequency generator using the HMSIW forward coupler resonator. Finally, Section 5 concludes the article.

2 | DESIGN OF FORWARD COUPLER CONFIGURATION

Two types of coupling can occur, forward coupling and backward coupling, when two microstrip transmission lines come closer. The backward coupling supports the TEM wave propagation and is suitable for low-frequency applications. The forward coupling, which works for a non-TEM environment is

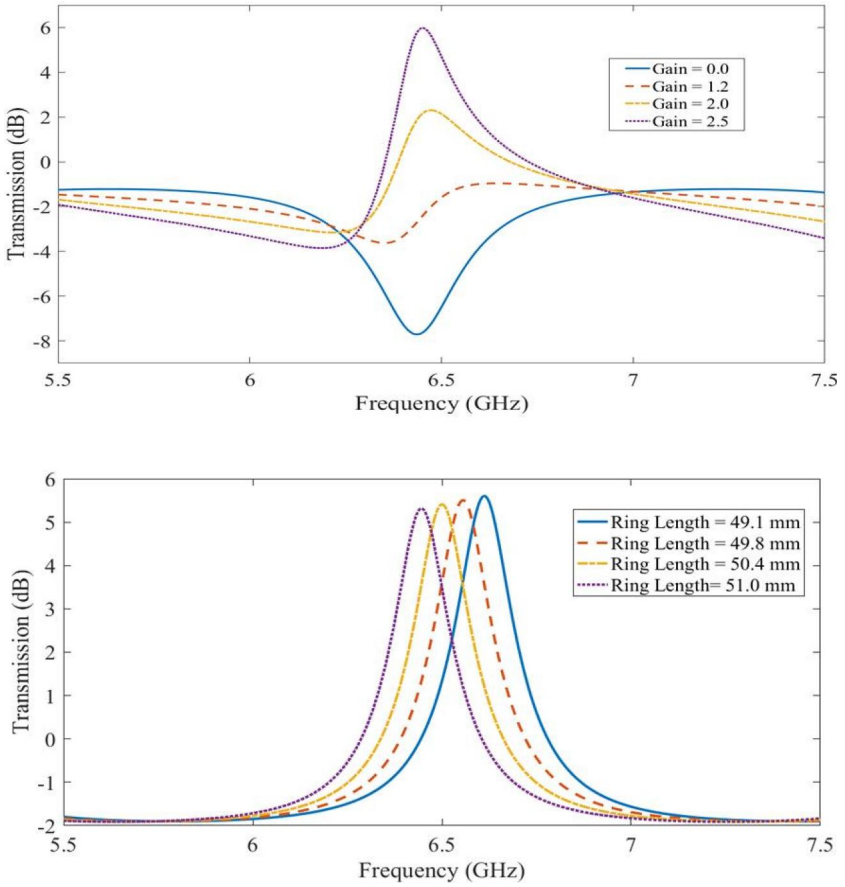

FIGURE 4 Parametric analysis of two-port forward coupler ring variable gain (ring length = 49.1 mm; up) ring length (at gain = 2.5 dB; below)

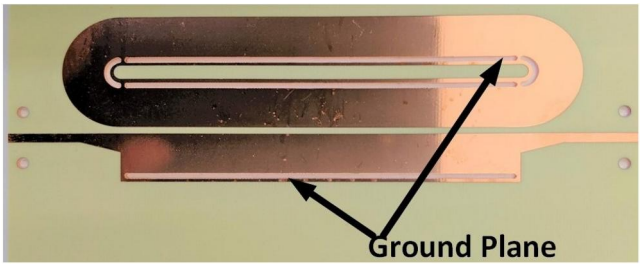

FIGURE 5 Fabricated Half-Mode Substrate Integrated Waveguide (HMSIW) forward coupler

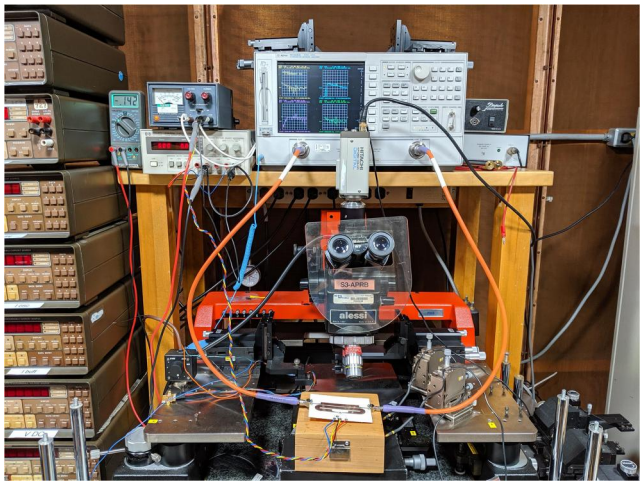

FIGURE 6 Measurement setup for the developed passive and active forward coupler resonators and frequency generator

used as a waveguide, and is appropriate for high-frequency applications and can also be used as a transmission line [22, 25]. Figure 2 depicts a typical signal flow graph for a four-port forward coupler. Its simple analysis results in $S_1 = -j \times \sin(kl)e^{-j\gamma l}$, $S_2 = \cos(kl)e^{-j\gamma l}$, $S_3 = 0$, and $S_4 = 0$. Here, k is the coupling per unit length, γ is the propagation constant, and l is the coupled length [26]. The scattering matrix of this forward coupler is given in (1).

A two-port forward coupler ring can be made by connecting port 3 (isolated port) and port 4 (coupled port) of the coupled lines, as shown in Figure 2. Its scattering matrix is given in (2) and clearly the $b_4 = a_3e^{-j\phi}$ and $b_3 = a_4e^{-j\phi}$, with ϕ being the phase loss due to length of the ring, are the updated values as the ports 3 and 4 are connected. The transmission response of the forward coupler ring in (3) can be found using the updated S-matrix in (2). Furthermore, the gain element inside the forward coupler ring, as shown in Figure 3, modifies the passive forward coupler ring's transmission response to (4). Here, G is the gain of the active element inside the passive ring of the forward coupler.

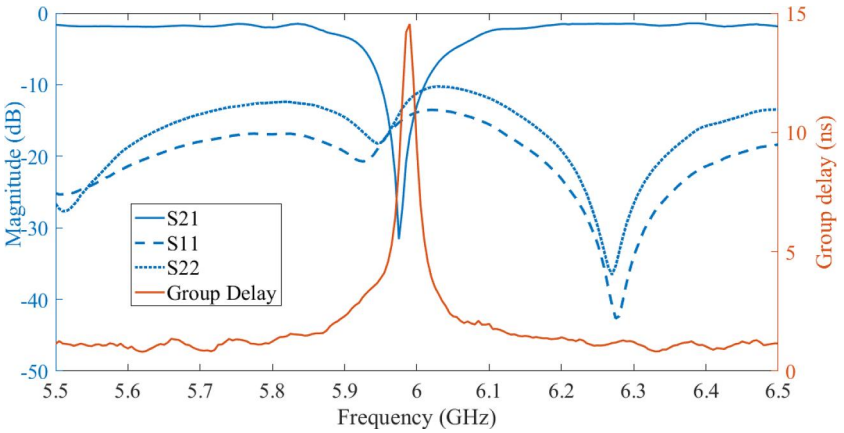

FIGURE 7 Measured S-parameters and group delay response of the passive Half-Mode Substrate Integrated Waveguide (HMSIW) resonator

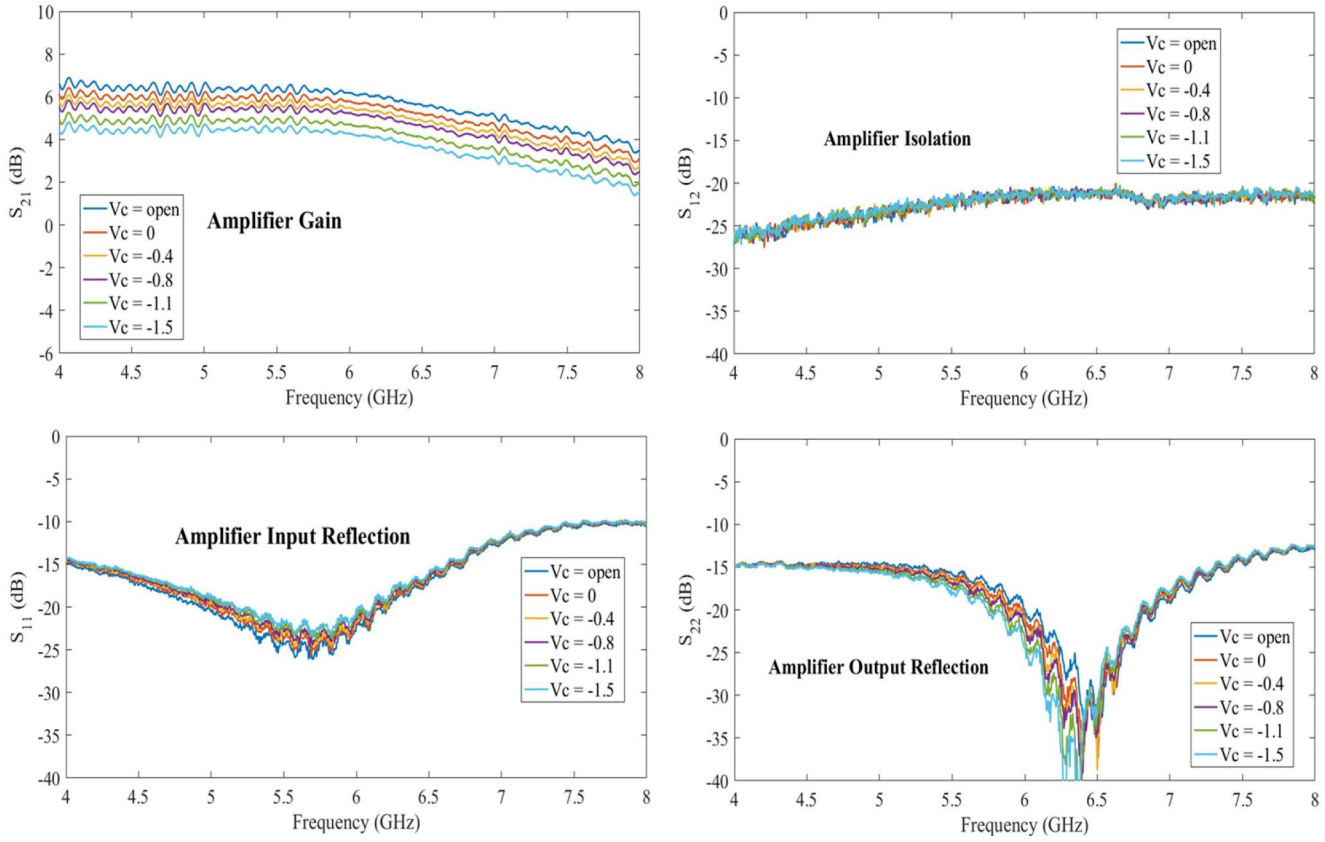

FIGURE 8 Measured biased amplifier S-parameters for active forward coupler structure

$$\begin{bmatrix} b_1 \\ b_2 \\ b_3 \\ b_4 \end{bmatrix} = \begin{bmatrix} 0 & S_2 & 0 & S_1 \\ S_2 & 0 & S_1 & 0 \\ 0 & S_1 & 0 & S_2 \\ S_1 & 0 & S_2 & 0 \end{bmatrix} \begin{bmatrix} a_1 \\ a_2 \\ a_3 \\ a_4 \end{bmatrix} \quad (1)$$

$$\begin{bmatrix} b_1 \\ b_2 \\ b_3 \\ b_4 \end{bmatrix} = \begin{bmatrix} 0 & S_2 & 0 & S_1 \\ S_2 & 0 & S_1 & 0 \\ 0 & S_1 & 0 & S_2 \\ S_1 & 0 & S_2 & 0 \end{bmatrix} \begin{bmatrix} a_1 \\ a_2 \\ b_4 e^{j\phi} \\ b_3 e^{j\phi} \end{bmatrix} \quad (2)$$

$$T = \left(S_2 + \frac{S_1^2 e^{j\phi}}{1 - S_2 e^{j\phi}} \right) \quad (3)$$

$$T' = \left(S_2 + \frac{S_1^2 e^{j\phi}}{1 - G * S_2 e^{j\phi}} \right) \quad (4)$$

The simulated transmission response of the forward coupler ring without and with the gain element is given in Figure 4. A parametric study was performed to investigate the ring length and gain effects on the proposed forward

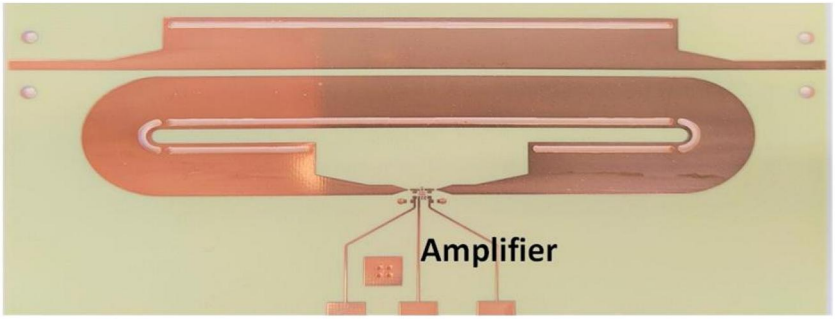

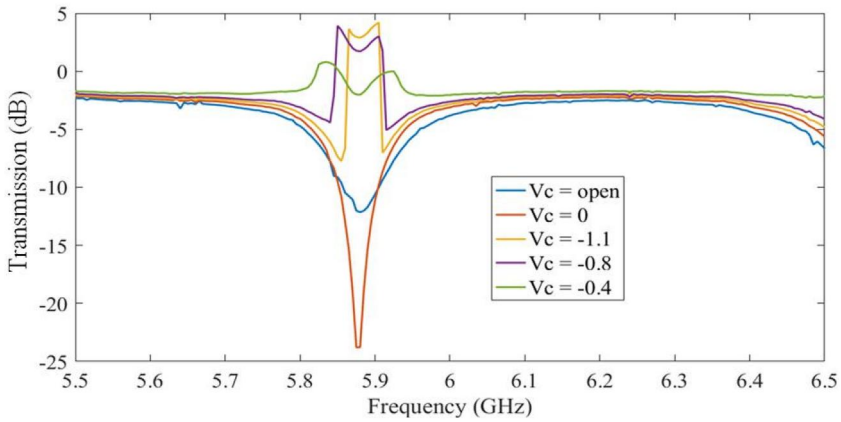

FIGURE 9 Active forward coupler with an amplifier inside the ring (up). Its measured transmission response at different amplifier bias (below)

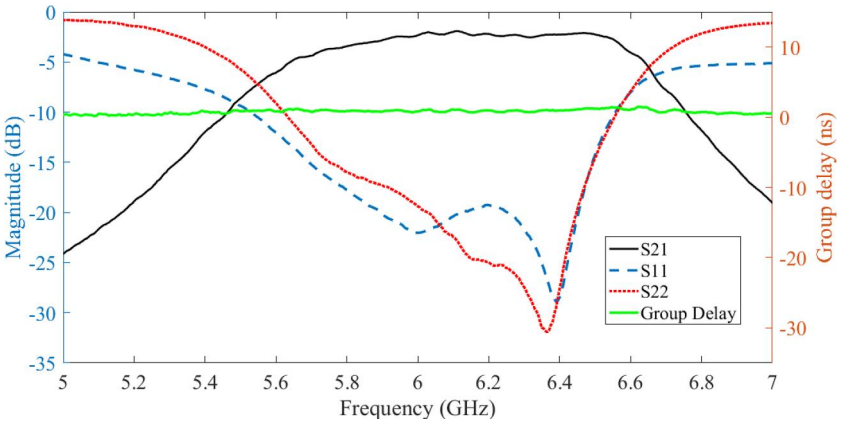

FIGURE 10 Measured S-parameters and group delay of the filter

coupler ring's transmission response. It is shown that the losses due to the coupled section of the structure can be compensated by an additional gain element inside the coupled section. Also, the length of the ring affects the resonating frequency of the coupled section as shown in Figure 4.

3 | MEASUREMENT AND ANALYSIS OF HMSIW FORWARD COUPLER RESONATOR

Substrate Integrated Waveguide with an imaginary magnetic wall and each half of the SIW structure becomes an HMSIW structure. The original field distribution is the same in both half parts of the structure because of its large width-to-height ratio and supports the same guided wave modes in the half structures. As reported earlier, HMSIW exhibits improved performance and low attenuation at higher frequencies supporting half-width of the SIW structure, making the overall structure compact [24]. It is now used to implement the proposed configuration shown in Figure 5. The length and width of the HMSIW structure are calculated using the waveguide concept for TE_{10} mode given in (5). Here, c is the speed of light, m, and n are the mode numbers, and a and b are the width and length of the waveguide, respectively.

$$f = \frac{c}{2\pi}\sqrt{\left(\frac{m\pi}{2a}\right)^2 + \left(\frac{n\pi}{2b}\right)^2} \tag{5}$$

The passive HMSIW configuration is fabricated on Rogers 3006, and the respective length of the coupled section and ring lengths are 21 and 48 mm. The sidewall of the fabricated structure makes ground by connecting the top metallic layer of the Rogers substrate to the ground with vias, as shown in Figure 5. The measurement setup is given in Figure 6, whereas the measured responses are given in Figure 7. The result indicates a positive group delay at around 5.98 GHz while showing excellent transmission behaviour.

Subsequently, the active forward coupler is realised. For such a situation, a gain element is used inside the ring to mitigate the losses due to the coupled structure. The measured profiles for multiple biasing conditions of the amplifier used in the active forward coupler are given in Figure 8. The fabricated active forward coupler using Rogers 3006 substrate is shown in Figure 9a. Once again, the setup in Figure 6 used to measure this design provides measured transmission response given in Figure 9b for different biasing of the amplifier. As the biasing of the amplifier changes, the gain of the amplifier changes accordingly, which affects the transmission response of the active forward coupler. Initially, for Vc open and Vc = 0, the losses due to the coupled structure are very high (−10 to −15 dB). At Vc = −0.4, amplifier gain equalises the losses of the coupled structure, and after that, the forward coupler shows gain in the transmission response, which saturates after a specific amplifier biasing voltage.

Apparently, there are frequency spurs outside the frequency of interest. Therefore, a 4-coupled microstrip transmission line section is used as a filter on both ends of the active forward coupler structure to eliminate the unwanted frequency outside the desired frequency band. The S-parameter and group delay response of the filter is given in Figure 10, and these indicate that the allowed passband of the filter is 1 GHz (5.7–6.7 GHz) and has a minimal loss (−4 dB) due to the filter. Finally, the prototype of the forward coupler, including 4-section filters on both ends of the active unit to eliminate unwanted signals outside the desired band, is shown in Figure 11.

For further tuning the system's frequency, a phase shifter can be introduced inside the ring according to the block diagram in Figure 12a. A number of simulations are carried out to assess the phase shifter effect on the performance, and the outcome is given in Figure 12b. The transmission responses show that with the increase in phase shift, the

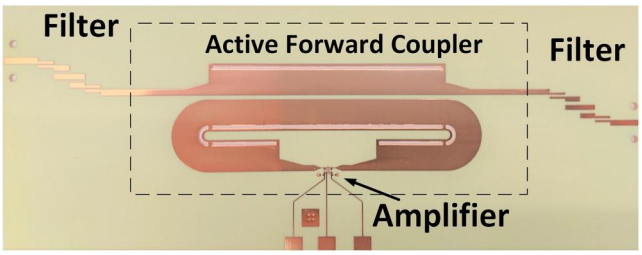

FIGURE 11 2-port active forward coupler with filters on both ends

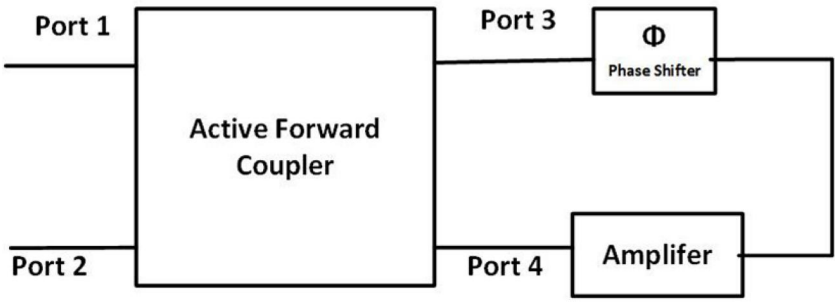

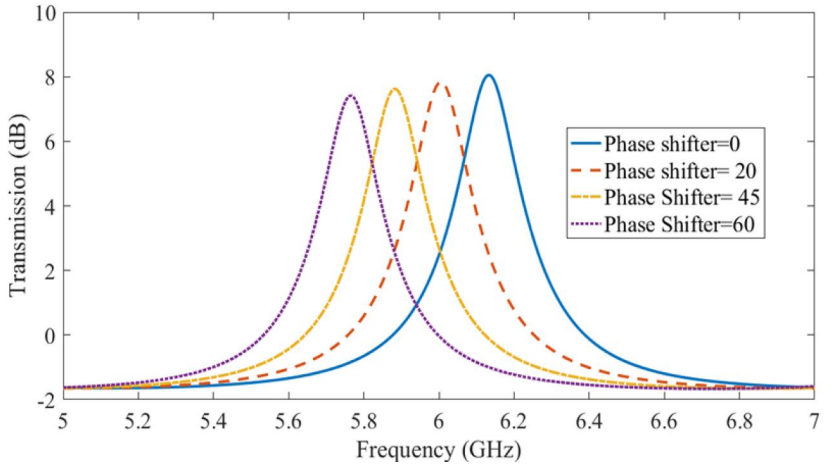

FIGURE 12 Block diagram for tuning the frequency using phase shifter (up). Simulation responses of the active forward coupler with variable phase shift (below)

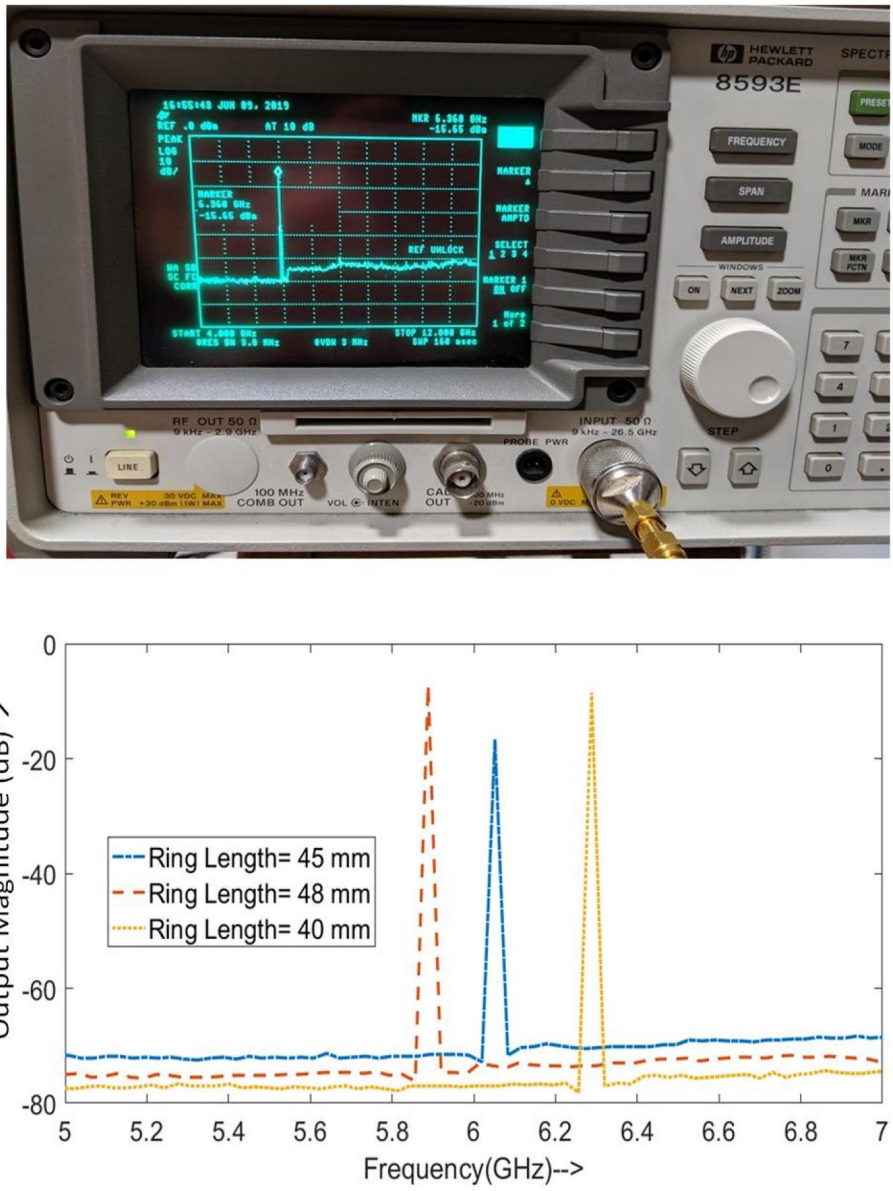

FIGURE 13 Output spectrum of active forward coupler structure with one end of the structure matched and closed. Spectrum analyzer response (up), responses of the spectrum analyzer for variable ring length (below)

frequency of the system decreases and vice versa. It can thus be inferred that the proposed design can be used to tune the system's frequency. Furthermore, the phase shifter can be used inside the forward coupler ring as well as an outside block. Thus, it provides flexibility to adjust the system after the fabrication.

4 | MEASUREMENT AND ANALYSIS OF ACTIVE HMSIW STRUCTURE FREQUENCY GENERATOR

The input port of the active forward coupler with filter is terminated in 50−Ω, and its output port is connected with the Agilent spectrum analyzer based setup in Figure 6. The amplifier noise works as an input signal for the frequency generator inside the forward coupler ring. The noise gets amplified due to the forward coupler ring at the dominating positive group delay resonating frequency. The spectral response of the fabricated active forward coupler ring with the tuned amplifier is shown in Figure 13a. The spectrum analyzer responses for variable ring lengths are given in Figure 13b.

It has been observed that the oscillation frequency of the frequency generator is close to the measured resonating frequency of the active and passive forward coupler transmission responses. Also, the phase noise of the generated frequency is calculated using the same spectrum analyzer. The sideband power is −52 dB at a 100-kHz offset for 0 dB carrier power. The losses due to different components are −10 dB adjusted in the oscillation frequency's carrier power and sideband power. The resolution bandwidth 1 kHz is considered, and phase noise is calculated using (6) [27], and it comes around

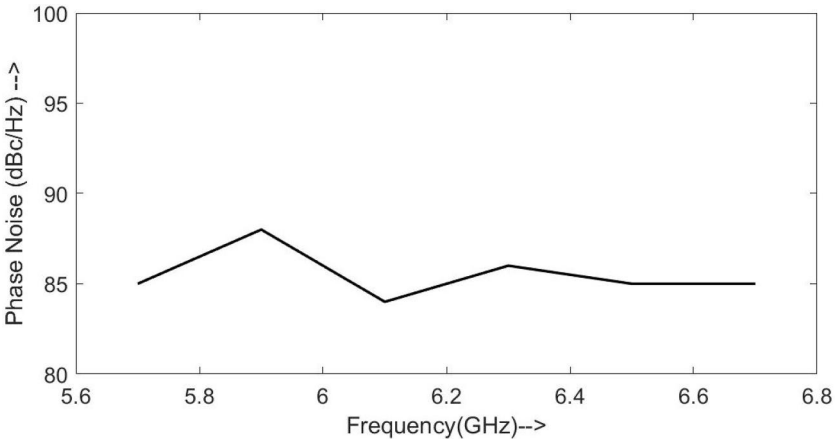

FIGURE 14 Measured phase noise (magnitude) at 100-kHz offset for different frequencies

TABLE 1 A comparison of the proposed frequency generator with previous proposed architectures

Oscillator	Operating frequency	Phase noise (dBc/Hz)	Size (mm)
SIW [14]	12 GHz	−73	48 × 12
SIW [20]	7.5 GHz	NA	45 × 10
SIW [19]	35.5 GHz	−90	8 × 6
This paper	5.9 GHz	−88	24 × 14

−82 dBc/Hz after considering all the losses. Therefore, the measured phase noise of the HMSIW frequency generator is better than 80 dBc/Hz at an offset frequency of 100 kHz over the entire tuning frequency range, as shown in Figure 14. A detailed comparison based on phase noise and board size between the proposed frequency generator and the previous proposed SIW based frequency generators given in Table 1 shows the superior behaviour of the proposed design.

$$P_{noise} = P_{sideband} - P_{carrier} - 10 * log(RBW)dB \quad (6)$$

5 | CONCLUSION

An active forward coupler for frequency generator is proposed, analysed, and experimentally validated in this paper. The forward coupler works on the concept of non-TEM, and hence it can be used for high-frequency applications. The proposed design can be used for chipless RFID readers to further reduce the size of RFID systems and chipless tags without incurring additional losses. The experimental results display the spectrum response of the frequency generator owing to amplifier noise inside the active forward coupler ring. The results demonstrate that the proposed frequency generator has the potential for use in low-cost chipless RFID readers.

ACKNOWLEDGMENT

This work was supported in part by the Nazarbayev University Collaborative Research Program (CRP) under Grant 021220CRP0222 and in part by the Nazarbayev University Faculty-Development Competitive Research Grants Program (FDCRGP) under Grant 110119FD4515.

CONFLICT OF INTEREST

No.

PERMISSION TO REPRODUCE MATERIALS FROM OTHER SOURCES

No.

DATA AVAILABILITY STATEMENT

Data sharing is not applicable to this article as no new data were created or analysed in this study.

ORCID

Vijay Sharma https://orcid.org/0000-0002-4800-8576
Mohammad Hashmi https://orcid.org/0000-0002-1772-588X

REFERENCES

1. Sharma, V., Malhotra, S., Hashmi, M.: Slot resonator based novel orientation independent chipless RFID tag configurations. IEEE Sensor. J. 19(13), 5153–5160 (2019)
2. Hashmi, M., Sharma, V.: Design, analysis, and realization of chipless RFID tag for orientation independent configurations. J. Eng. 5, 189–196 (2020)
3. Brinker, K., Zoughi, R.: Chipless RFID tags as microwave sensors for delamination detection in layered structures. In: 2021 IEEE International Instrumentation and Measurement Technology Conference (I2MTC), pp. 1–6. IEEE (2021)
4. Zheng, L., et al.: Design and implementation of a fully reconfigurable chipless RFID tag using inkjet printing technology. In: IEEE International Symposium on Circuits and Systems, pp. 1524–1527 (2008)
5. Koswatta, R.V., Karmakar, N.C.: A novel reader architecture based on UWB chirp signal interrogation for multiresonator-based chipless RFID tag reading. IEEE Trans. Microw. Theor. Tech. 60(9), 2925–2933 (2012)
6. Al-Tamimi, K.M., et al.: VCO-based ADC with built-in supply noise immunity using injection-locked ring oscillators. IEEE Trans. Circuits Syst. II: Express Br. 66(7), 1089–1093 (2018)
7. Elwakil, A.S.: Design of non-balanced cross-coupled oscillators with no matching requirements. IET Circuits, Devices Syst. 4(5), 365–373 (2010)
8. Sharma, V., Hashmi, M.: On the seamless integration and co-existence of chipless RFID in broad IOT framework. IEEE Access. 9, 69839–69849 (2021)

9. Lucarini, V., et al.: Kramers-Kronig relations in optical materials research, vol. 110. Springer Science & Business Media (2005)
10. Abdolrazzaghi, M., Daneshmand, M.: Exploiting sensitivity enhancement in micro-wave planar sensors using intermodulation products with phase noise analysis. IEEE Trans. Circuits Syst. I Regul. Pap. 67(12), 4382–4395 (2020)
11. Jarndal, A.H., Bassal, A.M.: Compact GAN class-ab Armstrong oscillator for resonant wireless power transfer. IET Circuits, Devices Syst. 13(2), 233–238 (2019)
12. Adhikari, S., et al.: Simultaneous electric and magnetic two-dimensionally tuned parameter-agile SIW devices. IEEE Trans. Microw. Theor. Tech. 61(1), 423–435 (2012)
13. Entesari, K., et al.: Tunable SIW structures: antennas, VCOS, and filters. IEEE Microw. Mag. 16(5), 34–54 (2015)
14. Cassivi, Y., et al.: Low-cost and high-q millimeter-wave resonator using substrate integrated waveguide technique. In: European Microwave Conference, pp. 1–4. IEEE (2002)
15. Chen, Z., et al.: Design of high-q tunable SIW resonator and its application to low phase noise VCO. IEEE Microw. Wireless Compon. Lett. 23(1), 43–45 (2012)
16. Bozzi, M., Georgiadis, A., Wu, K.: Review of substrate-integrated waveguide circuits and antennas. IET Microw., Antennas Propag. 5(8), 909–920 (2011)
17. Wu, K.: Integration and interconnect techniques of planar and non-planar structures for microwave and millimeter-wave circuits-current status and future trend. In: Asia-Pacific Microwave Conference, vol. 2, pp. 411–416. IEEE (2001)
18. Ranjan, R.K., et al.: High-frequency floating memristor emulator and its experimental results. IET Circuits, Devices Syst. 13(3), 292–302 (2019)
19. Zhong, C., et al.: Ka-band substrate integrated waveguide gunn oscillator. IEEE Microw. Wireless Compon. Lett. 18(7), 461–463 (2008)
20. Abdolhamidi, M., Shahabadi, M.: X-band substrate integrated waveguide amplifier. IEEE Microw. Wireless Compon. Lett. 18(12), 815–817 (2008)
21. Cassivi, Y., Wu, K.: Low cost microwave oscillator using substrate integrated waveguide cavity. IEEE Microw. Wireless Compon. Lett. 13(2), 48–50 (2003)
22. Nazemi-Rafi, H., Movahhedi, M.: Dispersive delay structure using cascaded-coupled CRLH-CRLH C-sections. Int. J. RF Microw. Computer-Aided Eng. 29(7), e21715 (2019)
23. Izquierdo, B.S., et al.: Substrate-integrated folded waveguide slot antenna. In: IEEE International Workshop on Antenna Technology: Small Antennas and Novel Metamaterials, pp. 307–309. IEEE (2005)
24. Hong, W., et al.: Half mode substrate integrated waveguide: a new guided wave structure for microwave and millimeter wave application. In: Joint 31st International Conference on Infrared Millimeter Waves and 14th International Conference on Teraherz Electronics, pp. 219. IEEE (2006)
25. Reed, J., Wheeler, G.J.: A method of analysis of symmetrical four-port networks. IEEE Trans. Microw. Theory Tech. 4(4), 246–252 (1956)
26. Mongia, R.K., et al.: RF and microwave coupled-line circuits. Artech house (2007)
27. Ip, K.H., Kan, T.M.Y., Eleftheriades, G.V.: A single-layer CPW-fed active patch antenna. IEEE Microw. Guid. Wave Lett. 10(2), 64–66 (2000)

How to cite this article: Sharma, V., Hashmi, M.: Frequency generator demonstration using half mode Substrate Integrated Waveguide (SIW) structures for chipless Radio Frequency Identification (RFID) reader. IET Circuits Devices Syst. 16(5), 410–418 (2022). https://doi.org/10.1049/cds2.12113